Mine Water and the Environment (2022) 41:748–763
https://doi.org/10.1007/s10230-022-00877-4

TECHNICAL ARTICLE

Assessment of Dewatering Requirements and Dewatering Well Design for an Open Pit Coal Mine in Central Anatolia

Ayse Peksezer-Sayit[1] · **Hasan Yazicigil**[1]

Received: 17 April 2021 / Accepted: 4 May 2022 / Published online: 25 May 2022

Abstract

The Çeltikçi Coal Basin is a newly discovered coal basin in Central Anatolia where 11 years of open-cut mining has been planned. The bulk of the mining will be conducted below the regional water table; hence, determination of the dewatering requirements and proper design of the dewatering wells plays a critical role. This study (i) defined the dewatering requirements of the open-pit mine, (ii) established a dewatering well design for the area, and (iii) assessed the anticipated impacts of the dewatering activities. For this purpose, a 3-D numerical groundwater flow model was developed using the FEFLOW software. Yearly dewatering requirements were determined under transient conditions. For the dewatering well simulations, two types of dewatering wells were considered: permanent wells located at the open pit boundary that would increase in number as the excavation proceeds and wells located at the periphery of the yearly excavated area that would be operational for about two years. The simulation results indicated that 894 wells were required to satisfy dry working conditions; the average pumping rate throughout the mine life was calculated as 322 L/s. The impacts of open-pit dewatering on groundwater resources were assessed in terms of spring discharge and base flow rates in the nearby Kirmir stream. As a result of dewatering, most of the village water supply springs and fountains will dry up in the area. In addition, the base flow rates to the Kirmir stream will be decreased by 15%.

Keywords FEFLOW · Numerical modeling · Çeltikçi coal basin · Groundwater inflow

Introduction

Water is an essential component during a mine's life cycle. A lack of water in the mining area may lead to water supply problems in the construction and operational periods. Meanwhile, encountering water may also be a critical issue, since it delays operations and causes economic and safety problems (Aryafar et al. 2009; Connelly and Gibson 1985; Fernandez-Rubio and Lorca 1993; Morton and Mekerk 1993; Williamson and Vogwill 2001). To satisfy safe and dry working conditions, dewatering requirements should be determined in advance, even at the pre-feasibility stage (Ardejani et al. 2003).

Both analytical and numerical methods are widely utilized to assess dewatering requirements. Analytical methods are often used at the planning stage of the mine life cycle. These methods are based on simplifying assumptions and serve as an easy-to-use informative tool (Fontaine et al. 2003; Marinelli and Niccoli 2000; Singh and Atkins, 1985). They generally provide a preliminary approach to predict the groundwater inflow rate to mine excavations. On the other hand, numerical models can simulate complicated situations arising from the complexity of the actual system and mine design. Thus, numerical models can provide more realistic results and are widely used to assess dewatering requirements (Ardejani et al. 2003; Bochenska et al. 2000; Brouyere et al. 2009; Peksezer-Sayit et al. 2015; Rapantova et al. 2007; Unsal and Yazicigil 2016; Zaidel et al. 2010). The selection of model dimension (1-D, 2-D, or 3-D models) as well as modeling methods (finite difference, finite element, or finite volume) depends on various factors, including the geological and hydrogeological conditions of the site, type of mining, the scale of the problem domain, and the experience of the modeler (Adams and Younger 2001; Anderson et al. 2015). Once the groundwater inrush rate to the open pit

✉ Ayse Peksezer-Sayit
aysepeksezer@gmail.com

[1] Department of Geological Engineering, Middle East Technical University, 06800 Ankara, Turkey

is defined, an efficient dewatering system must be designed to remove this excess water in order to continue mining. Based on the hydrogeological characterization of the system, common methods can be used, ranging from horizontal or vertical drains to dewatering wells (Argunhan-Atalay et al. 2021; Younger et al. 2002).

Although dewatering is a prerequisite for mining below the regional water table, groundwater drawdown can cause significant stress on the environment. The drawdown caused by the mining activities can alter the regional water balance and impact the existing water resources and natural wetlands (Ardejani et al. 2003; Booth 2006; Brunetti et al. 2013). Furthermore, once the mining activities cease, the groundwater levels will start to rise and create a pit lake if the area is not backfilled (Castendyk and Eary 2009; Unsal and Yazicigil 2016). A complete understanding of the hydrogeological system is required to anticipate the impact of dewatering on water resources.

Based on the hydrogeological characteristics of the area, the simulated groundwater inrush rates into the mine excavations and the actual amount of groundwater withdrawal from the system may not overlap. This difference can arise from the positioning of the dewatering wells, their locations with respect to each other, and the hydraulic properties of the system. Dewatering wells are generally located at the periphery of the excavated areas so as not to hinder mining activities. On the other hand, numerical simulations calculate groundwater inrush rate to the open pit from the entire mining area. Therefore, even at the pre-feasibility stage, a dewatering design should be implemented to obtain a more realistic time-wise groundwater withdrawal rate from the pit area. In this study, dewatering requirements and dewatering well design were applied at an open pit lignite mine. The mining progress addressed herein does not have a regular trend, i.e. the traditional cone-shaped excavation method is not implemented in the area due to the areal distribution of the coal layers, which increases the complexity of the numerical simulations and well design.

This paper aims to: (i) define the dewatering requirements of an open-pit coal mine located in central Turkey, (ii) establish a dewatering well system design for the area, and (iii) assess the anticipated impacts associated with the dewatering activities. For this purpose, a 3-D numerical groundwater flow model was developed. Also, the impact of dewatering wells on the groundwater system was assessed in terms of the base flow rate of Kirmir stream and springs and community water supplies.

Study Area

The study area is located in central Anatolia, approximately 50 km northwest of Ankara, the capital of Turkey. In terms of hydrology, it is bounded by the Çamlıdere dam reservoir in the north and Kurtboğazı dam reservoir in the east, covering an area of 602.5 km^2. The study area is situated between UTM coordinates of 446,900–475,000 easting and 4,452,300–4,478,900 northing (Fig. 1). The main surface waters within the study area are Kirmir and Pazar streams, flowing in northeast-southwest and north–south direction, respectively. The topographic elevations range from 760 to 780 m along the Kirmir stream to 1820 m along the watershed divide at the northern part of the area. Based on the pre-feasibility studies, about 37 million tonnes of coal is planned to be extracted.

The area has a continental climate with higher humidity due to its vicinity to the Black Sea region. It is characterized by hot and dry summers and snowy winters; most of the precipitation is observed in winter and spring. The long-term average annual precipitation value for the study area was determined as 392.4 mm (Yazicigil et al. 2014). Mean monthly temperature values show seasonality, where July and August are the hottest months (mean temperature values are above 20 °C), whereas the temperature values are below zero in winter.

The geology of the study area include, from oldest to youngest, a succession of volcanic basement rocks, Miocene siliciclastics, Plio-Quaternary units, and Quaternary alluvium. The Miocene strata, were grouped under the name of "Çeltikçi" formation. The Çeltikçi Formation is composed of the Bostantepe, Lower Çavuşlar, Upper Çavuşlar, Abacı, Kocalar, Aktepe and Bezci members (AMM 2015). The coal seams are found at the lower parts of the Upper Çavuşlar member (Fig. 2).

The volcanic basement rocks are composed of lava flows, tuffs, and andesitic-basaltic pyroclastics, which are unconformably overlain by the Çeltikçi Formation. The lowest part of the Çeltikçi Formation is characterized by the Bostantepe member, which includes fluvial siliciclastics composed of sandstones and conglomerates. These lithologies are overlain by the Lower Çavuşlar member, consisting of oolitic limestone, varve, thin-bedded immature coal seams, tuff, and silicified claystone. In the western part of the area, the Lower Çavuşlar member unconformably rests on the volcanics. The Lower Çavuşlar member passes to the Upper Çavuşlar member upwards in the sequence, with an alternation of claystones, bituminous mudstones and lignite seams. These are overlain by the Abacı member, characterized by a single ignimbrite layer. The Abacı member is topped by the Kocalar member, which is mainly made up of siliciclastics grading into the Aktepe member consisting of limestones.

These lithologies are overlain by the Bezci member, characterized by siliciclastic sandstones and conglomerates. The overlying Plio-Quaternary units are characterized by recent alluvial fans, terrace deposits, alluvium, and talus (Fig. 3).

The structural geology of the study area is dominated by thrust and normal faults. The normal faults generally strike NE-SW and dip towards the NW (AMM 2015). The fold axes display a similar trend to the faults, extending in a NE-SW direction (Fig. 3).

Pit Information

Eleven years of mining has been planned in the study area. The pit extends 1.9 km in the N–S and 2.7 km in the E–W direction. The pit area is bounded by faults at the north (the Kirmir 2 fault) and south (the Karatas fault). Also, the Kirmir stream passes the northern edge of the pit; the distance between the Kirmir stream and northern boundary of the open pit ranges between 50 and 350 m.

According to the mine plan, the maximum excavation depth will range from 70 to 104 m throughout the operational period. Mining will start at the southern part of the open pit and proceed towards the north. The northwestern part of the pit forms the deepest portion. The yearly mining activities are shown in Fig. 4, which shows the excavation areas corresponding to each year. As can be seen from the sequence of excavated areas, the mining operations do not obey the traditional cone-shaped mine development. According to the pre-feasibility studies, previously excavated areas will be backfilled except for year 11. The observed groundwater levels indicate that within the open pit, the depth to water table values ranges from artesian conditions to 100 m below ground surface (bgs) at the northeastern part. Hence, throughout the mining process, the pit bottom is generally located below the water table, which makes dewatering inevitable.

Hydrogeological Characterization

The hydrogeology of the study area was determined based on information from the field studies, monitoring and pumping wells, and discharges from springs and fountains. 67 monitoring wells were drilled to determine hydrogeological conditions and hydraulic parameters and to monitor the groundwater level and quality. In addition to these wells, nine large diameter pumping wells were drilled to measure groundwater elevation or pressure, and discharge rates (Fig. 5). Also, aquifer tests (pumping, recovery, slug, and free flow tests) were conducted to determine the hydraulic properties (Yazicigil et al. 2014, 2015a, b).

During the field studies, 70 springs and fountains were identified within the study area, and the discharge rates and field parameters were monitored (Fig. 5). The springs in the study area are mainly used for water supply purposes. The measured discharge rates of the springs are low, with average rates between 0.002 and 1.82 L/s. Typically, the discharge rates of the springs increase in the winter and peak during springtime, which is followed by a dry or low flow period during the summer (Yazicigil et al. 2014, 2015a).

To test the hydraulic properties of various rock units in the study area, each well was screened within the target formation and sealed off from the other units. The hydraulic properties of the Bostantepe member could not be tested due to an insufficient number of wells drilled in that unit. Constant discharge pumping tests, followed by recovery tests, were conducted on seven pumping (PW-1, PW-3, PW-5, PW-6, PW-7, PW-8, PW-9) and 10 monitoring wells (PW-9A, CEL19A, CEL47, CEL47A, CEL53A, CEL59, CEL59A, CEL59B, CEL107, CEL107A). At PW-4A, a free-flow test and at PW-2 a slug test were applied. Slug tests were also conducted at 13 monitoring wells (CEL25, CEL36, CEL43, CEL44, CEL49, CEL50, CEL51, CEL52, CEL61, CEL64, PW-8A, CEL-93A, and CEL89C). The hydraulic properties, indicating minimum, maximum, and average values based on each unit, are summarized in Table 1. The composite hydraulic conductivity and storativity values obtained from wells screened at more than one geologic unit are also given in Table 1. In the study area, the maximum hydraulic conductivity values are observed in the alluvium, which is followed by Lower Çavuşlar claystones and Upper Çavuşlar coal measures. The geometric mean of the hydraulic conductivity values calculated for the Upper aquifer (i.e. Aktepe and Kocalar members), Upper Çavuşlar member, and the volcanics give similar results. The storativity values in the study area are generally low and were determined for the coal measures, Upper, and Lower Çavuşlar members (Yazicigil et al. 2014, 2015a).

Conceptual Model

Based on the information gathered from field studies, the area has three aquifers, namely the Upper, Lower, and Alluvium aquifers. The volcanics, together with the Bostantepe, Lower and Upper Çavuşlar members, form the Lower Aquifer in the study area. The second important aquifer in the study area includes the Kocalar, Aktepe, and Bezci members separated from the Lower Aquifer by the silicified tuff layer. These units form the Upper Aquifer in the study area, which is an unconfined aquifer developed in a synclinal basin. The Quaternary-aged alluvial deposits observed along the Pazar and Kirmir streams form an unconfined aquifer. However, the limited areal extent and thickness of the alluvium reduce the yield of the Alluvium Aquifer (Yazicigil et al. 2015a).

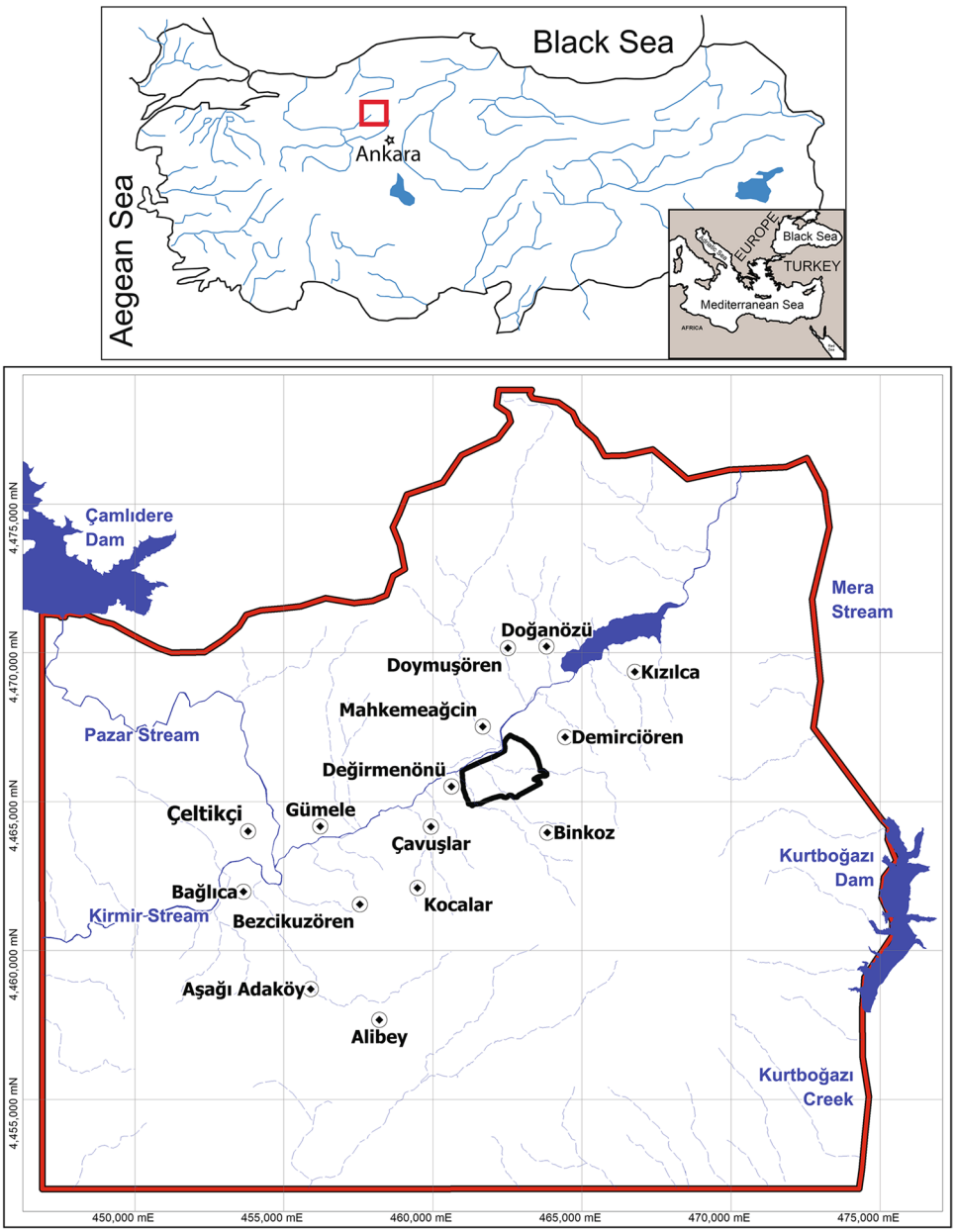

Fig. 1 Location map of the study area

The Lower Aquifer has a confined character below the Upper Aquifer (at the western part of the Kocalar 2 fault) and is unconfined elsewhere. The sudden changes in topography also produce free-flow conditions in the Lower Aquifer. The presence of a silicified, massive tuff layer at the bottom of the Abacı Ignimbrite forms an impervious boundary above the Upper Çavuşlar member and results in the formation of confined conditions. Hence, at the western part of the Kocalar 2 fault, an upper unconfined aquifer is underlain by a confined lower aquifer. The schematic representation of the hydrogeological system in the study area is shown in Fig. 6.

A groundwater elevation map was only prepared for the Lower Aquifer due to an insufficient number of monitoring wells drilled in the Upper and Alluvium Aquifers (Fig. 5). In the vicinity of the planned mine site, the groundwater flow in the Lower Aquifer is generally towards the Kirmir stream. The hydraulic head varies from 1150 m at the southeastern part of the area towards 800–850 m along the Kirmir stream. Faults located in the southern part of the Kirmir stream control groundwater flow in those locations. At the northern part of the Kirmir stream, the groundwater flows towards the Pazar and Kirmir streams.

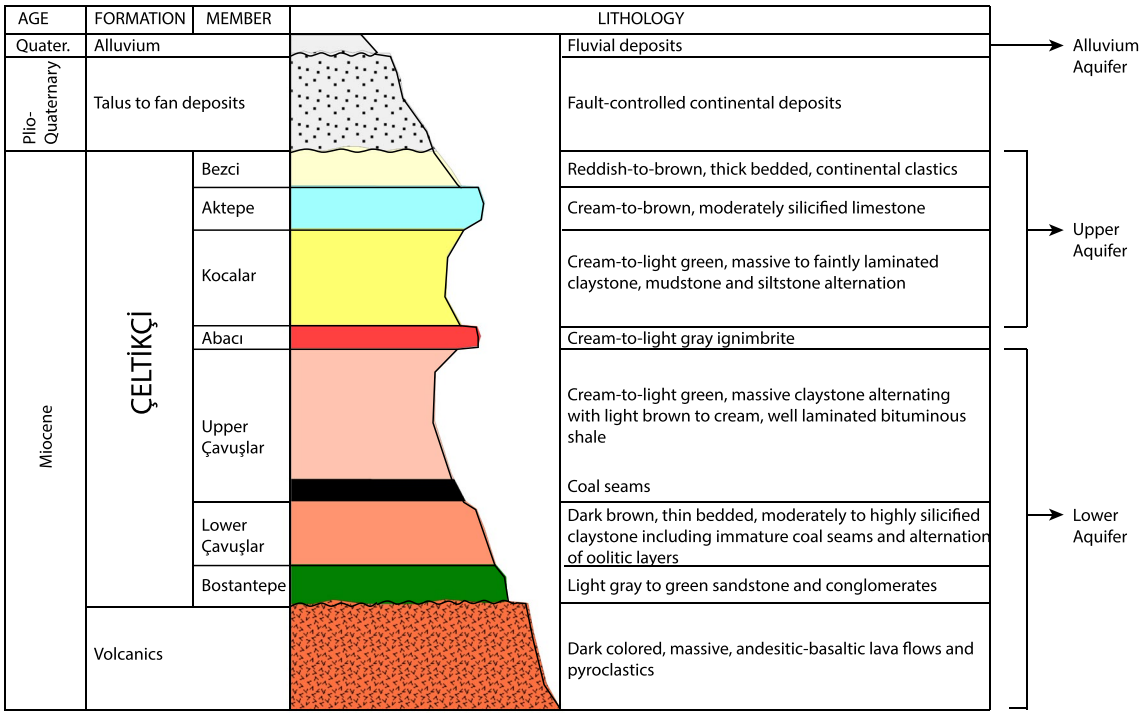

Fig. 2 Stratigraphy and generalized lithological profile of the region

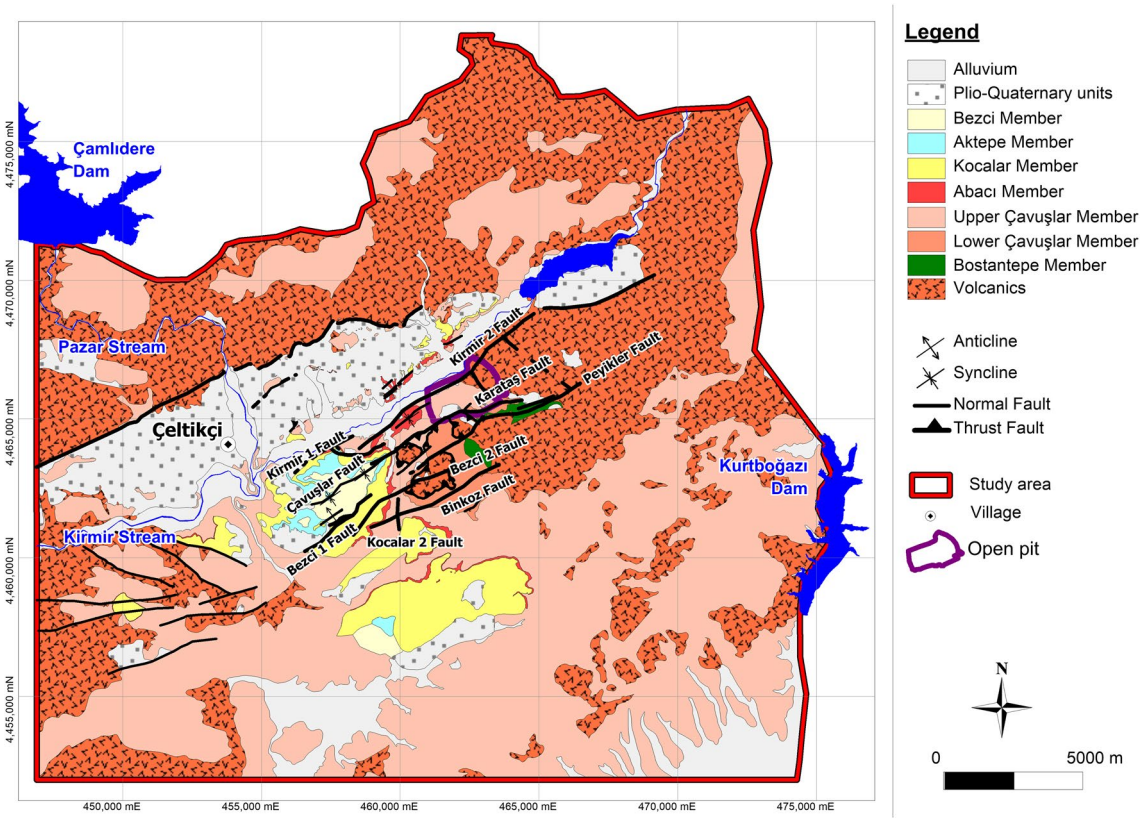

Fig. 3 Geological map of the study area

Fig. 4 Yearly progress of open pit

Groundwater Flow Model

A 3-D groundwater flow model of the study area was set up via FEFLOW 7.0 software (DHI-WASY 2015). It solves the governing equations of flow, mass, and heat transport in porous and fractured media using the finite element method for saturated and unsaturated conditions. The model domain covers an area of 602.5 km^2. It is bounded by the Çamlıdere Dam Reservoir and the watershed divide in the north, the Kurtboğazı Dam Reservoir and streams/creeks located at the upstream (Mera stream) and downstream part of this dam (Kurtboğazı creek) in the east (Fig. 7). The south and west boundaries are located ≈ 14 km away from the planned open-pit, providing enough distance to avoid any boundary effect. The extent of the model grid in the N–S and E–W directions are 26.8 and 28.7 km, respectively. The model domain consists of 16 layers and 17 slices. The topographic surface is represented by slice 1, where the elevation ranges between 1820 and 755 m. Slice 17 has a uniform elevation of 0 m. For the domain of interest, the well logs were used to define the thicknesses of lithological units, which were then interpolated to obtain a domain-wise distribution of layers.

The finite element mesh contains 2,965,242 nodes and 5,570,944 elements (Supplemental Figure S1). A mesh refinement was applied to the open pit and its vicinity to better simulate mining activities. Hence, the element sizes applied to the model range from 10 to 30 m near the planned mine area and reach 500 m at the periphery of the model domain. In the model domain, mesh quality was checked by (i) Delaunay criteria and (ii) maximum interior angle of

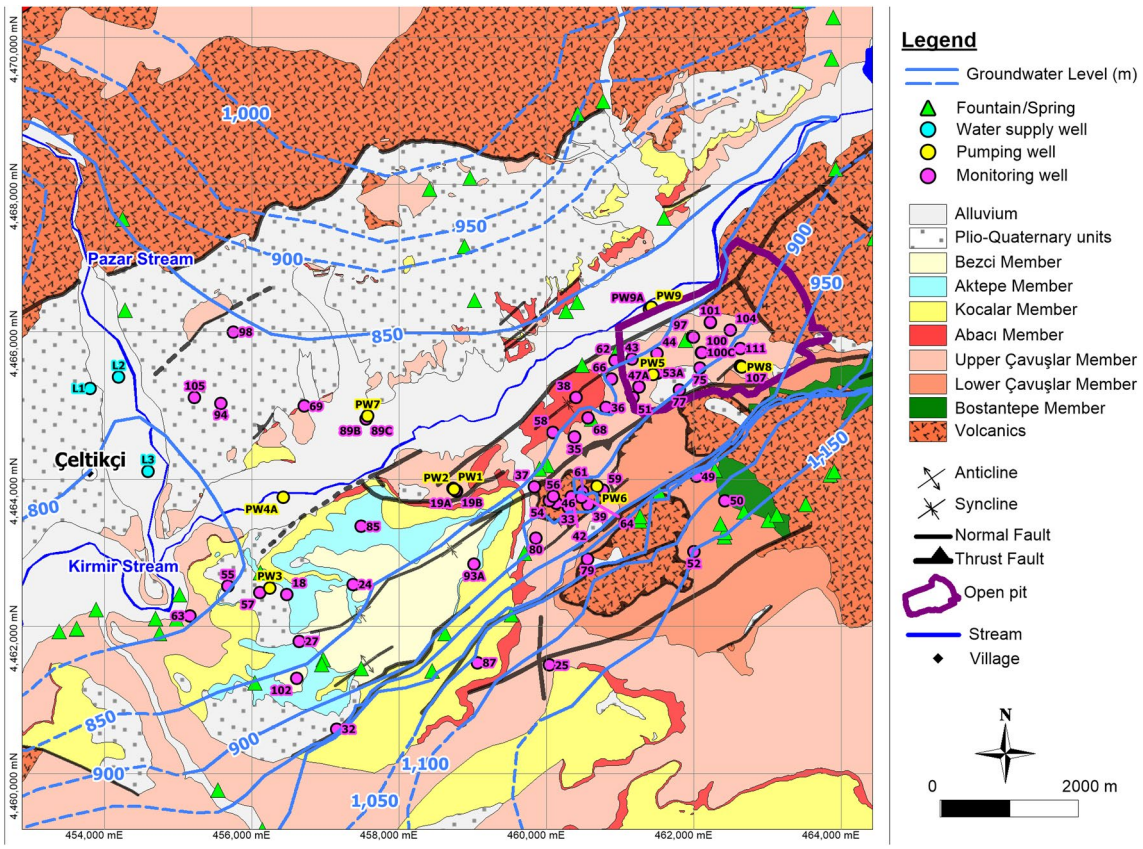

Fig. 5 Hydrogeological map of the study area

Table 1 Calculated hydraulic conductivity and storativity parameters of the geological units

	Hydraulic Conductivity, K (m/s)			Storativity, S			No. of Tested Wells
	Min	Max	Geo. Mean	Min	Max	Geo. Mean	
Alluvium	4.27×10^{-6}	5.59×10^{-5}	1.36×10^{-5}	–	–	–	3
Aktepe and Kocalar Members	2.66×10^{-8}	1.42×10^{-6}	2.11×10^{-7}	–	–	–	2
Upper Çavuşlar Member	1.31×10^{-8}	1.55×10^{-6}	1.17×10^{-7}	3.15×10^{-4}			5
Coal	1.26×10^{-7}	2.26×10^{-6}	6.78×10^{-7}	2.16×10^{-5}	1.54×10^{-4}	4.41×10^{-5}	5
Lower Çavuşlar Member	5.52×10^{-9}	7.59×10^{-5}	1.17×10^{-6}	2.24×10^{-5}	8.92×10^{-2}	4.89×10^{-3}	10
Volcanics	4.89×10^{-9}	2.86×10^{-5}	2.08×10^{-7}	–	–	–	6
Alluvium and Upper Çavuşlar Member	6.16×10^{-8}	9.21×10^{-5}	1.61×10^{-5}	1.72×10^{-2}	9.43×10^{-1}	6.12×10^{-2}	2
Coal and Lower Çavuşlar Member	3.09×10^{-7}	1.22×10^{-6}	7.45×10^{-7}	1.37×10^{-4}	1.16×10^{-2}	1.58×10^{-3}	2

triangles, where all the elements obey the Delaunay criteria, and the maximum interior angles of all triangles were also constrained to 120° to obtain stable results.

Initial and Boundary Conditions

Within the model domain, the surface water reservoirs of the Çamlıdere, Kurtboğazı, and Doğanözü dams were simulated by hydraulic head boundary conditions, where the hydraulic head equals 1000, 964, and 870 m, respectively. Throughout the model domain, the intermittent streams and springs are represented by hydraulic head boundary conditions with the maximum flow rate constraint of 0 m^3/d to prevent any inflow to the groundwater system. Two main streams within the model domain i.e. the Kirmir and Pazar streams, as well as the Mera stream, which forms the eastern boundary, are simulated by a fluid transfer boundary condition. For the rest of the study area, no flow boundary condition was used.

The groundwater withdrawal resulting from drinking/irrigation water needs within the model domain is represented by a multi-layer well boundary condition. The hydrogeological studies reveal that 176 wells are used within the model domain for water supply purposes. The assigned pumping rates for these wells range from 0.05 to 44.30 L/s (Fig. 7).

The net infiltration to the model area was simulated by in/outflow on top/bottom material property in FEFLOW. The water budget calculations (in which the Thornthwaite (1968) method was used to calculate potential evapotranspiration and the SCS (1964) curve number was used for surface runoff determinations) reveal that the average annual groundwater recharge from direct precipitation in the study area is 55 mm, which comprises 14% of the annual precipitation. Since the study area is located in a steep and undulating topography, the distribution of groundwater recharge also varies within the study area. In this regard, assigned groundwater recharge values were distributed considering the median elevation of the model area.

The calculated hydraulic conductivity values, which were obtained from pumping and slug tests conducted at various pumping and monitoring wells, were exported to FEFLOW with minimal alteration (Supplemental Table S1). Nine different conductivity zones were determined based on the lithological characteristics and aquifer test results. On the other hand, the hydraulic properties of the fault zones were determined during model calibration (Supplemental Table S1). Within the model domain, the vertical to horizontal hydraulic conductivity ratio was set to 0.1 for all units, except for the fault zones, where the flow was assumed to be isotropic (Yazicigil et al. 2015a). The specific yield and specific storage values in the model domain were also determined based on the lithology of the units and aquifer test results. The specific yield for the alluvium was assumed to be 0.2. The pumping test conducted in PW-8, which is screened in the Upper and Lower Çavuşlar members and coal, was simulated under transient conditions to estimate the specific yield value for the model domain. The simulation results gave the best representation of the pumping test with values of 0.008, whereas the specific storage parameter was determined to be 3×10^{-5} m^{-1}.

Calibration

The model was calibrated under steady-state conditions to determine the initial conditions for the transient simulations. Then, transient calibration was conducted to obtain the storage parameters. During the calibration, initially assigned hydraulic conductivity values and boundary conditions were adjusted by trial and error to obtain an acceptable match between the observed and calculated groundwater levels. The calibrated hydraulic parameters used in the model are shown in supplemental Table 1. The average groundwater levels measured at 72 observation wells during the 2012–2015 period were used in the steady-state calibration. The performance of the model predictions were optimized between observed and calculated groundwater levels by minimizing the root mean square error (RMSE) and normalized root mean square error (NRMSE) at the observation wells. The model was calibrated with an RMSE of 16.09 m and NRMSE of 4.56%, indicating that the model is capable of simulating actual field conditions (supplemental Figure S2). In addition to the groundwater levels, the base flow to the Kirmir and Pazar streams and conceptual and calculated groundwater budgets were also compared. The average instantaneous flow rates observed in October at four flow monitoring points located along the Pazar stream (SW-11 and SW-12) and Kirmir stream (SW-1 and SW-16) were used (Fig. 5). The baseflow rate observed in October during 2012–2015 periods was determined as 0.03 m^3/s between SW-11 and SW-12, and 0.5 m^3/s between SW-1 and SW-16. The net groundwater discharge rate between these points was calculated as 0.033 m^3/s for SW-11 and SW-12, and 0.41 m^3/s for SW-1 and SW-16, which are compatible with the observed data. The areal distribution of the observed and calculated groundwater levels for the lower aquifer are provided in supplemental Figure S3, whereas the calibrated groundwater budget of the study area is shown in Table 2.

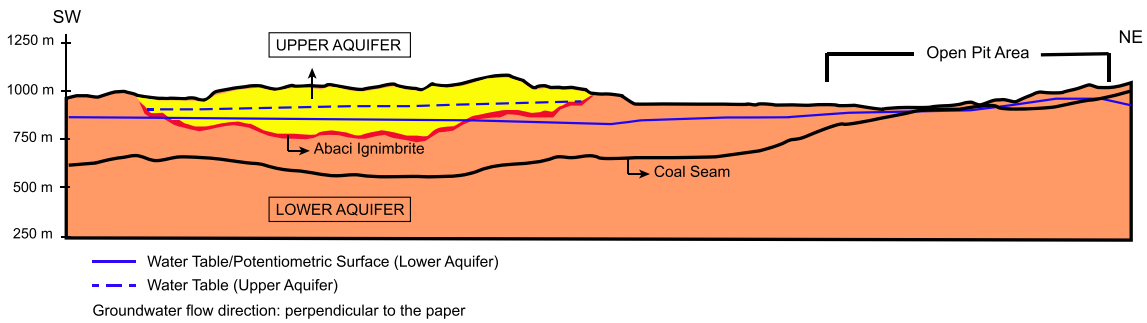

Fig. 6 Schematic representation of the hydrogeological system in the study area

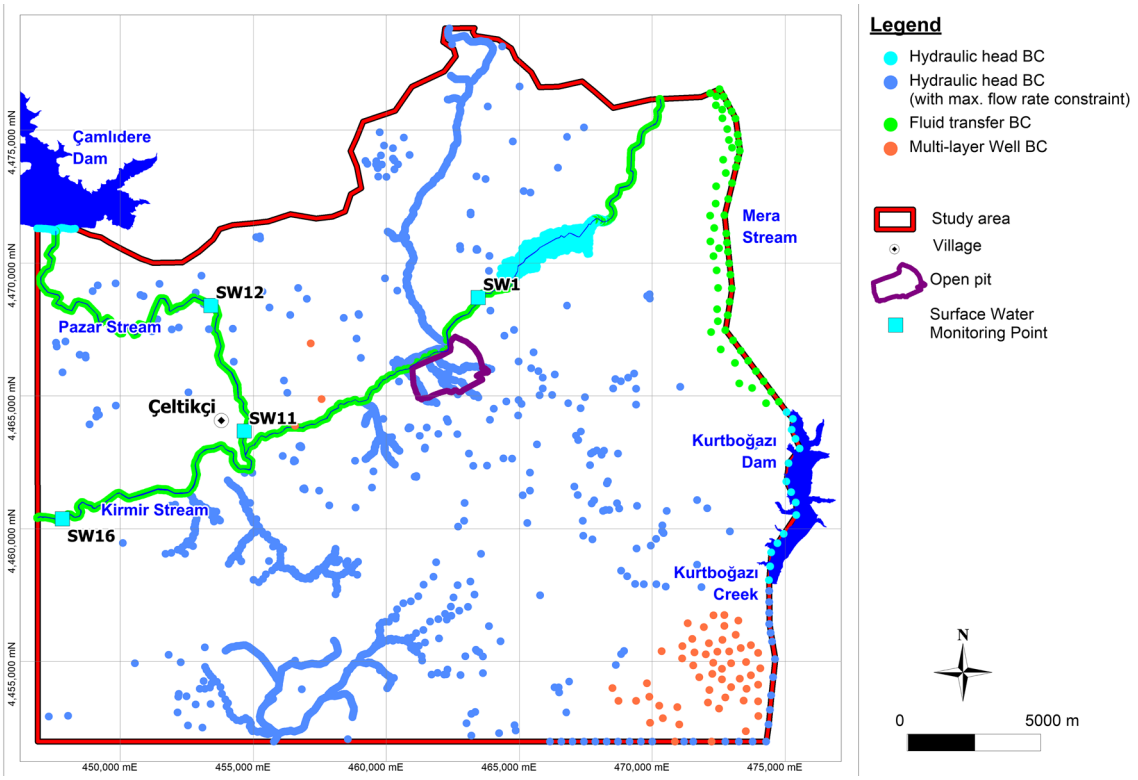

Fig. 7 Boundary conditions applied to the model (view from slice 1)

A sensitivity analysis was also performed to evaluate the uncertainties associated with the model parameters. For this purpose, a series of simulations were done, and the RMSE and NRMSE values were compared. The analyzed parameters include (i) hydraulic conductivity values assigned to the lithologies (supplemental Figure S4), (ii) recharge from precipitation (supplemental Figure S5), and (iii) hydraulic conductivity values assigned to the faults (supplemental Figure S6). These parameters were varied independently by multiplying the original values with the coefficients shown in the horizontal axes of supplemental Figs. 4 and 6, and the RMSE and NRMSE were calculated at the end of each simulation. The results indicate that the model was not sensitive to changes in the hydraulic conductivity values of the alluvium and Abacı Ignimbrite. Although the model is not sensitive to the decrease of hydraulic conductivity in the coal, Upper, and Lower Çavuşlar members, it shows high sensitivity to an increase of this parameter. For the Bostantepe member, volcanics, and model domain, the model is insensitive to changes in hydraulic conductivity values. The sensitivity of recharge from precipitation was determined by assigning different recharge values (55, 67, 84.4, and 100 mm/year). For the fault zones, although the lowest RMSE and NRMSE values were obtained when the hydraulic conductivity of Karataş fault was decreased by 10 times, the calibrated hydraulic conductivity value was kept unchanged to avoid any significant impact on dewatering simulations. The sensitivity analysis revealed that the parameters used in the calibrated model gave the lowest error values.

Dewatering Requirements

The calibrated groundwater flow model under steady-state conditions was transferred into the transient model to simulate open pit dewatering requirements. The storage parameters were obtained from the pumping test simulation conducted at PW-8 well during the calibration stage. The average annual recharge value was also converted into monthly recharge series, based on the monthly water budget calculations (Yazicigil et al. 2015a). Eleven years of mining were simulated by 132 30-day periods, with a total simulation time of 3960 days.

The amount of groundwater inflow rate into the open pit was simulated by drains, i.e. hydraulic head boundary conditions with maximum flow rate constraint. Since the mine plan is available on a yearly basis, the hydraulic head value for the drains was assigned to be equal to the pit bottom elevation for the corresponding year. The boundary condition was constrained by a maximum flow rate of 0 m^3/d to prevent any inflow to the groundwater system.

The yearly mining activity is shown in Fig. 4. According to the pre-feasibility studies, previously excavated areas will be backfilled except for year 11. For each year, the drains become active at the nodes located within the excavation area. Hence, the amount of groundwater inflow rate coming from these nodes to the pit was determined. The simulation results indicate that the average groundwater inflow to the pit will be 79 L/s. The effects of direct rainfall and surface water flow from the benches were not considered in the simulations.

The yearly integrated groundwater inflow rate to the pit was obtained from the model results (Fig. 8). According to the graph, the groundwater inflow rate to the pit starts at year 1 and peaks at year 11 (169 L/s). The increasing trend in the flux corresponds to progress in the pit excavation, whereas decreasing trends indicate less dewatering demand. The dewatering requirements increase continuously as the mine progresses in advance except for year 6, during which dewatering conducted at year 5 caused a lower dewatering requirement.

The prediction of groundwater inflow rate to the open pit is closely related to the hydraulic conductivity values assigned to the Kirmir 2 and Karataş faults, located at the northern and southern part of the open pit, respectively (Fig. 3). To observe the impacts of the hydraulic conductivity of the faults, simulations were repeated by increasing and decreasing the assigned hydraulic conductivity values 10 times compared to the base model (supplementary Figure S7). The simulation results indicate that the average groundwater inflow rates were calculated as 69 and 114 L/s, when the assigned hydraulic conductivity values were decreased and increased 10 times, respectively. On the other hand, the maximum inflow rate of 169 L/s was calculated as 131 and 223 L/s, when the hydraulic conductivity of the faults were decreased and increased 10 times, respectively.

Wells drilled in the open pit area and screened in the coal measures were used to check whether groundwater levels in the pit will be lowered to the desired levels as a result of dewatering. The simulated groundwater levels at wells PW-5, PW-8, CEL-53A, CEL-77, CEL-97A, CEL100C, CEL-101, and CEL-107 were compared to the pit bottom elevations at those points. The desired groundwater levels were obtained, satisfying dry working conditions in the open pit (Fig. 9).

Dewatering Well Design

To achieve dry working conditions, dewatering wells were designed to pump out the simulated groundwater inflow rate, and hence keep groundwater levels below the excavation depth. Mining in the open pit is planned to start at the southern border and continue in the northwestern direction (Fig. 4). The final mining activity is located in the northwest corner of the pit, where the deepest excavation is planned. Since the mine plans are available on a yearly basis, the wells were planned to be located at the periphery of the yearly excavated areas. However, in the northwestern part of the pit, due to (i) deepening of the excavations in years 9, 10, and 11, (ii) the closeness to the Kirmir stream, and (iii) the increase in excavation volume will require drilling of the dewatering wells within the open pit area.

In the dewatering well design, two groups of wells were simulated. Group 1 wells are permanent wells, which are located at the periphery of the open pit area. They will start to operate as mining advances from southeast to northwest and continue to pump throughout the life of the mine. Their numbers steadily increase from year 1 to 11. Group 2 wells are temporary wells, located at the periphery of the year's excavated area. They will start pumping one year prior to mining and continue to pump during operation within the corresponding area. These wells will only operate for two years.

During the pumping tests conducted in the open pit area (at wells PW-8 and PW-9), the average pumping rate from the wells was below 3 L/s. Hence, in the simulations, the pumping rate assigned to the dewatering wells is generally 1 L/s. However, the assigned pumping rates were increased to 2 L/s for the wells that will be drilled during the last four years of mining in order to lower the groundwater levels at the northwestern border where excavations will

Table 2 Calibrated groundwater budget for the study area

Boundary conditions	Budget component	RECHARGE (hm.^{3}/year)	Discharge (hm.^{3}/yearr)
Distributed Sink/Source	Recharge from precipitation	50.88	–
Cauchy BC	Kirmir and Pazar streams	6.83	34.04
	Mera stream	5.6	7.75
Dirichlet BC	Dams	7.86	7.85
	Springs	–	0.60
	Creeks	–	18.6
Well BC	Wells	–	1.82
TOTAL		71	71

approach the Kirmir 2 fault and Kirmir stream. In addition to the increased pumping rates, extra dewatering wells were added within the pit area, which will operate for the last two years of mining. All the wells are screened from 30 m below the ground surface to the bottom of the coal measures (i.e. slice 13 in the model). Based on the simulation results, a total of 894 wells are needed to ensure dry working conditions. The areal distribution of dewatering wells is given in Fig. 10, whereas the change of the number of active wells with respect to mine progress is provided in supplemental Fig. 8. The assigned and simulated pumping rates for each year are also compared in Fig. 11. For the first six years of mining, the assigned and simulated pumping rates are identical, whereas after year 6, simulated pumping rates start to decrease (Fig. 11). As the excavation continues, drawdown drops below the filtered depth of some permanent wells. Pumping from these wells cannot be modeled, which in turn results in overall lower pumping rates. The simulated total pumping rates from the wells increase from 60 to 735 L/s during advanced stages of mining. The average pumping rate was calculated to be 322 L/s.

To check whether the groundwater levels decrease to the desired elevations, groundwater levels and pit bottom elevations were compared along five sections (Fig. 12). Apart from section 1 and section 2, which pass through the finally excavated areas, groundwater levels were lowered to the desired elevations in all sections. For section 1 and section 2, due to the increase in the excavation depth and volume, and avoiding drilling of the wells within the excavation area, the groundwater levels were still slightly above the pit bottom elevation after dewatering.

Assessment of Dewatering Impacts

To achieve dry and safe working conditions, 894 dewatering wells will be required based on the simulation results. The impacts of dewatering were evaluated in terms of (i) the change to the Kirmir stream baseflow rate with respect to time and (ii) the areal distribution of the cone of depression resulting from dewatering.

In the calibrated model, the base flow rate of the Kirmir stream was calculated as 0.41 m^3/s for the section between the two instantaneous flow monitoring stations, i.e. SW-1 and SW-16 (Fig. 7). Due to the mine operations being so close to the stream, the impact of dewatering activities on the base flow rate was evaluated for the mentioned section on a yearly basis (supplemental Figure S9). The simulation results indicate that the base flow rate of the Kirmir stream will decrease about 15% as a result of drawdown during mining operations.

The spatial distribution of the cone of depression resulting from 11 years of dewatering is displayed in Fig. 13. According to this figure, the maximum amount of drawdown at the northwestern corner of the pit is 166 m, which decreases to 50 m at a distance of 1–1.5 km. The cone of depression is distorted by the presence of the fault zones within the study area. The mining induced drawdown also affects springs and community water supplies in the study area. If the model is valid, springs located within the 5 m drawdown contour are expected to dry out. In this context, 16 springs and two village water supply springs will dry out until mining ceases.

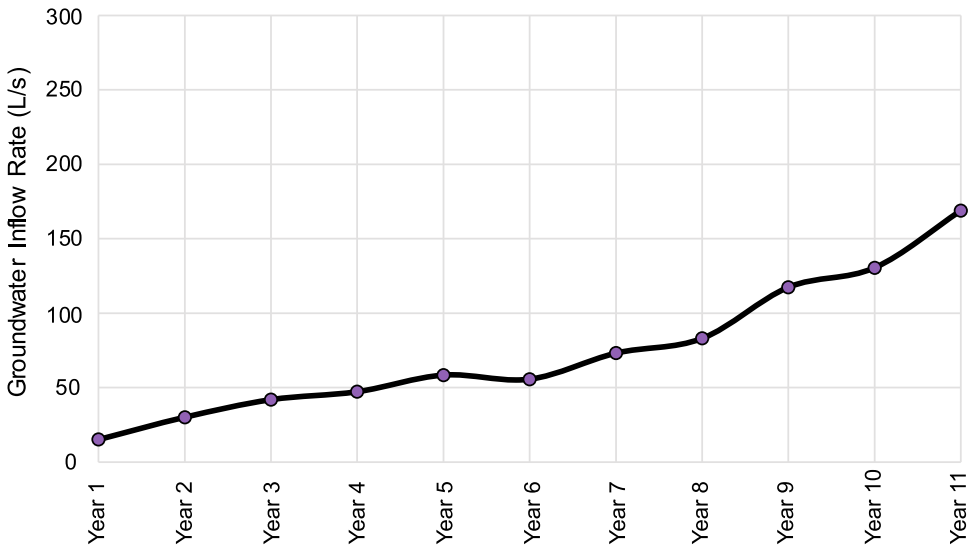

Fig. 8 Simulated groundwater inflow rate to the open pit

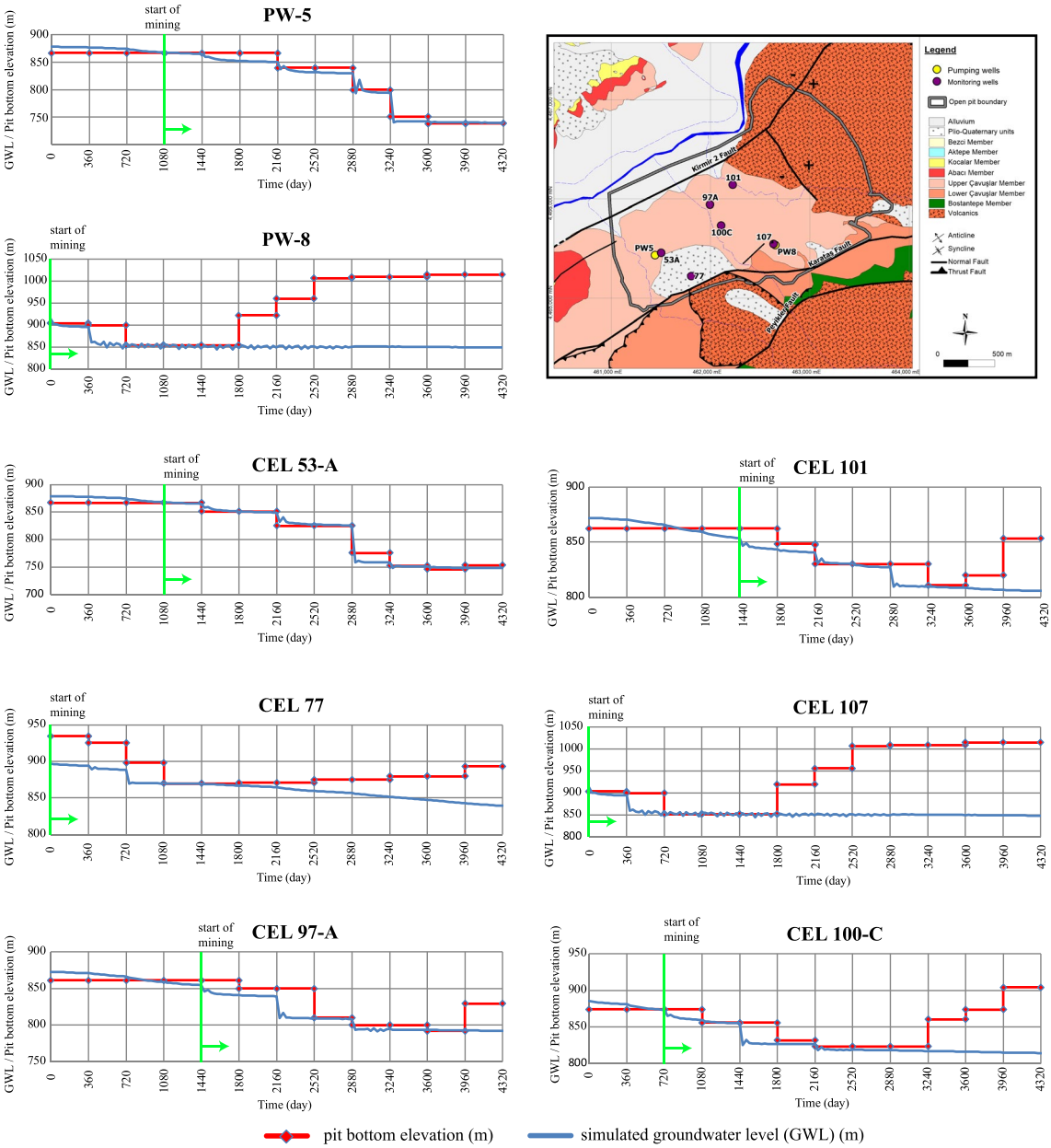

Fig. 9 Simulated groundwater levels and pit bottom elevations at the observation wells after open pit dewatering

Discussion and Conclusions

This study aimed to determine dewatering requirements for the Çeltikçi open-pit coal mine, prepare a dewatering well design, and assess the effects of dewatering on groundwater resources. In this regard, following a detailed hydrogeological characterization of the area, a 3-D groundwater flow model was set up and calibrated under steady-state conditions. Subsequently, the calibrated model was converted into a transient model to simulate the dewatering requirements. The presence of fault zones in the northern and southern part of the open pit and the proximity of the pit to the Kirmir stream posed some problems.

As mentioned earlier, the mine progress does not follow regular cone-shape geometry. The irregular excavation regime as well as the presence of fault zones, distribution of coal layer, and complex geology play a significant role in the selection of modeling code. In this regard, FEFLOW software is selected, where the finite element method is utilized. One of the critical points in the numerical models is the mesh design. Although smaller mesh sizes create more accurate results, they also increase the computing time. Therefore, an optimal size of 10–30 m for the area of

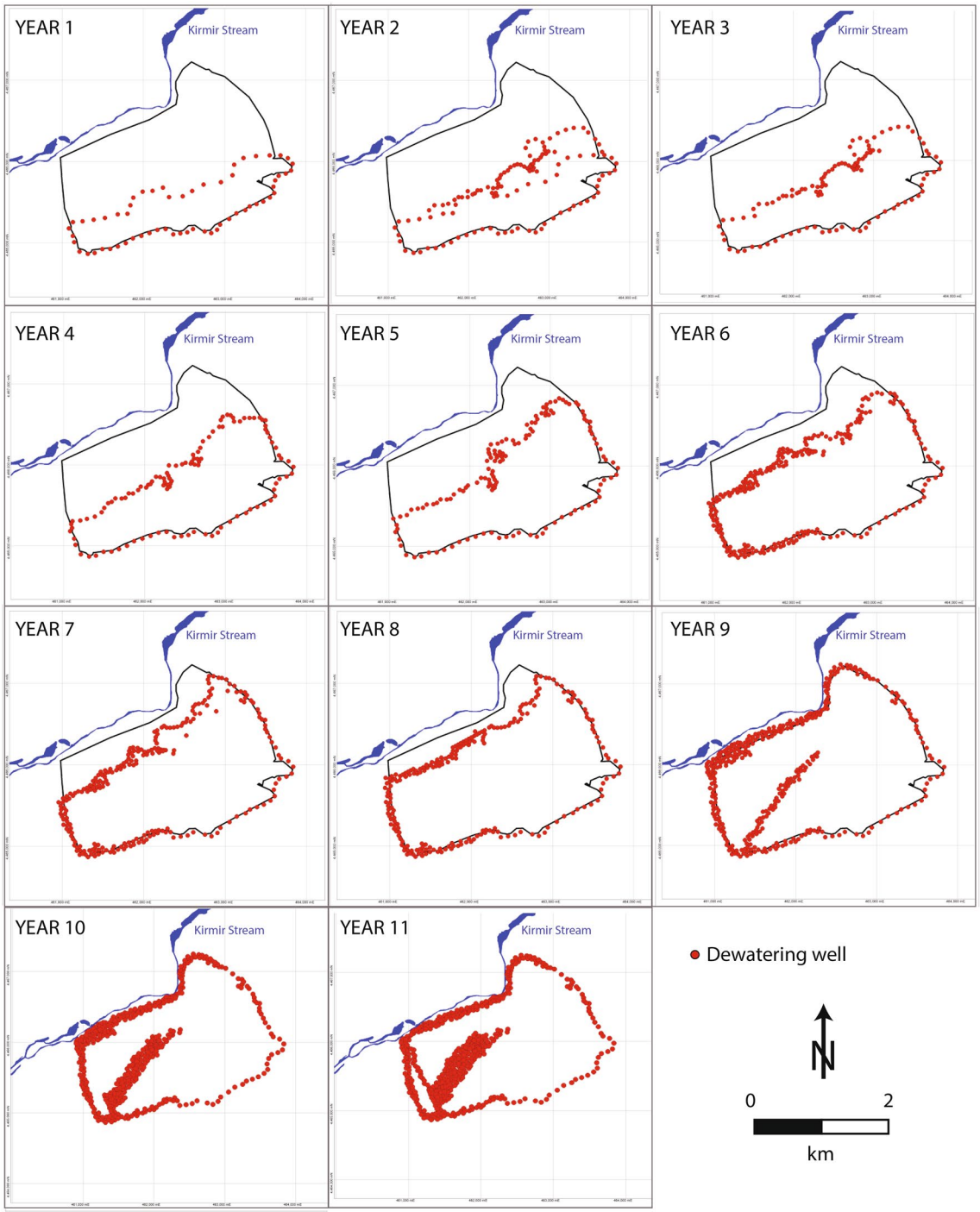

Fig. 10 Areal distribution of simulated dewatering wells

interest is selected. The main uncertainty associated with the groundwater flow model presented herein is the hydraulic conductivity of the fault zones. Although the hydraulic properties of the lithologies were tested in the field, the hydraulic properties of the fault zones were determined during model calibration. In this regard, sensitivity analyses were conducted to evaluate the uncertainties associated with the model parameters (i.e., hydraulic conductivity values assigned to the lithologies, recharge from precipitation, and hydraulic conductivity values assigned to the faults).

The dewatering requirements of the open pit and dewatering well design were simulated for the study area. The results indicate that the average groundwater inflow rate to the open pit is 79 L/s, which ranges between 15 L/s (year 1) to 169 L/s

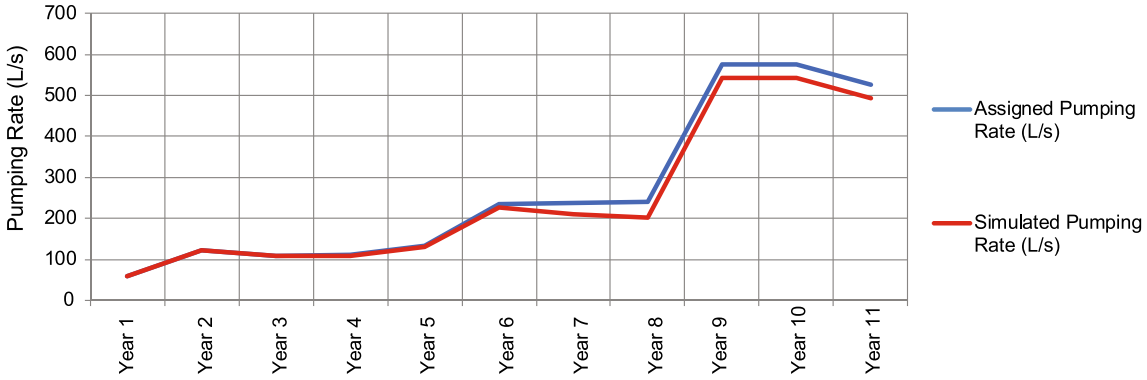

Fig. 11 Assigned and simulated total pumping rates to the dewatering wells

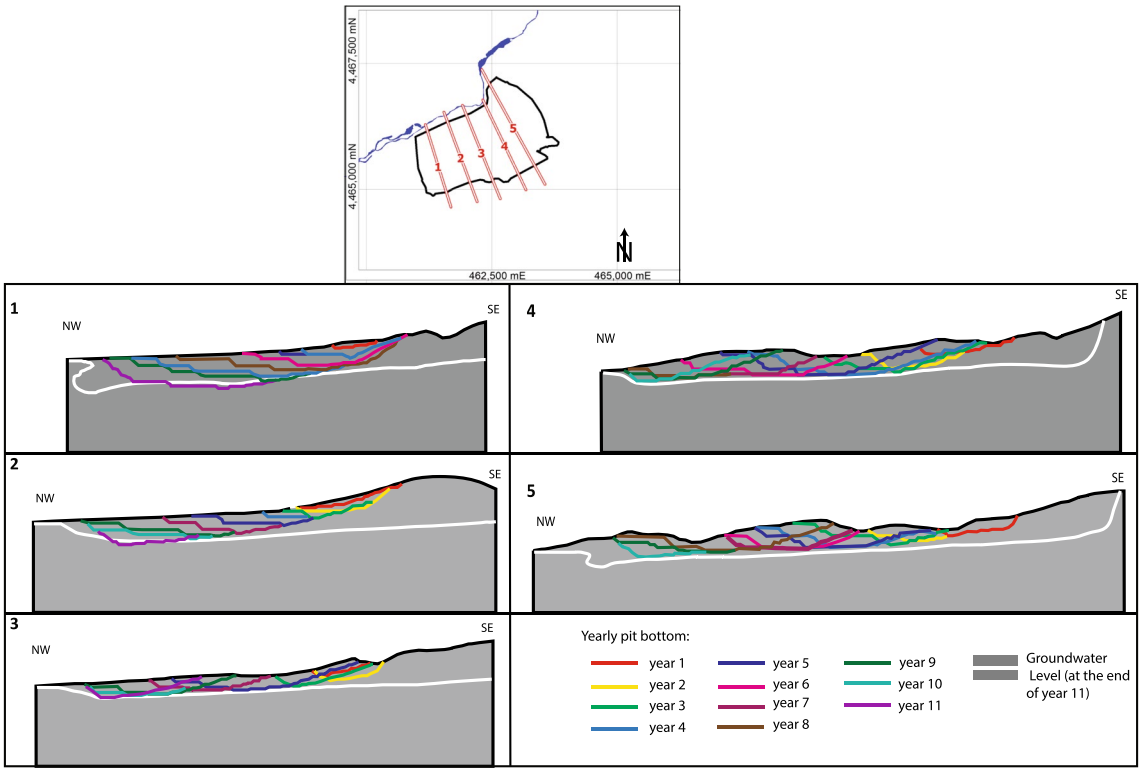

Fig. 12 Pit bottom and groundwater levels obtained as a result of dewatering well simulations along 5 cross-sections

(year 11). On the other hand, according to the dewatering well design, the simulated total pumping rates vary between 60 and 735 L/s, with an average 322 L/s. This highlights that the calculated dewatering requirements may be far different than those of the dewatering well design, which can be attributed to the hydrogeological characteristics of the site and the presence of the operational constraints. In determining dewatering requirements, the amount of groundwater inflow to the mine excavation is allowed from every node located within yearly excavation areas. On the other hand, in the dewatering well design, attention was paid to avoid drilling wells within the excavation area to allow continuous mining operations. Hence, avoiding the drilling of the wells within the excavation area and low hyrdaulic conductivities result in the simulation of elevated pumping rates from dewatering wells. It should be noted that determining dewatering requirements alone gives only preliminary information for any mine operations. Even at the pre-feasibility stage, a dewatering well design should be implemented to obtain a more realistic time-constrained groundwater withdrawal rate from the pit area.

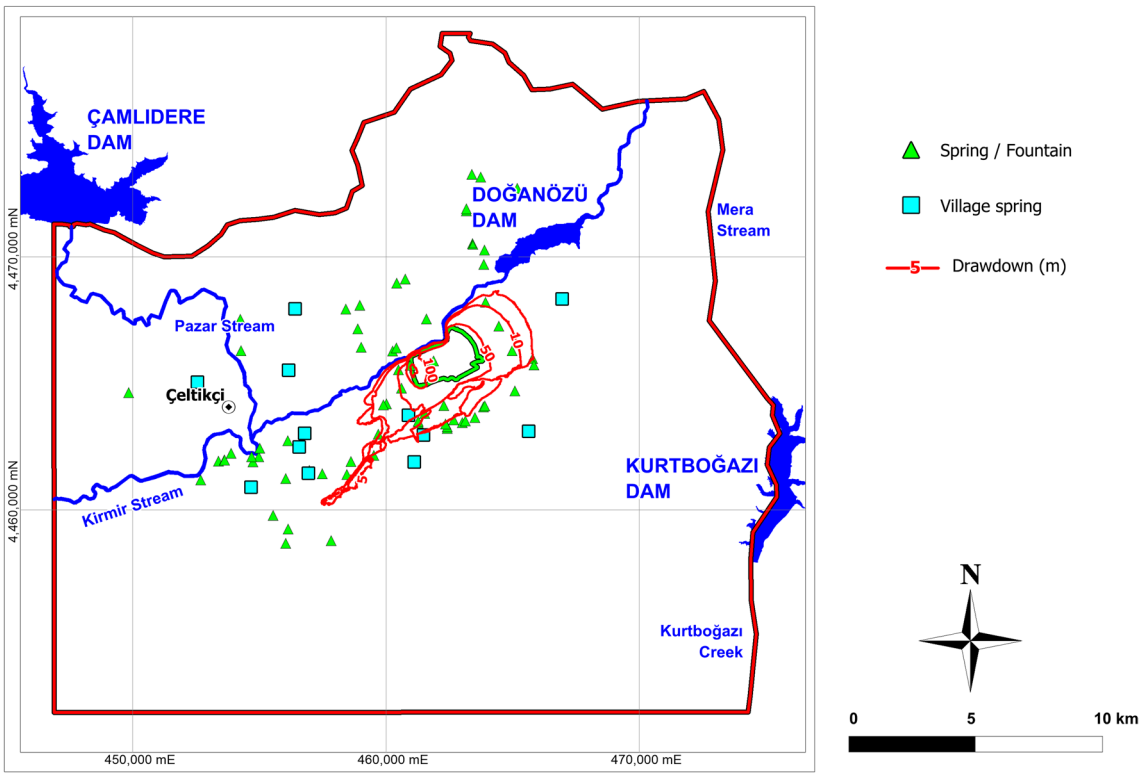

Fig. 13 The simulated drawdown contours at the end of 11 years of mining

The effect of dewatering wells on the groundwater system was also assessed. The simulation results show that about a 15% decline is expected for the base flow rate of the Kirmir stream as a result of drawdown. The decrease in the groundwater levels in the area also affects springs and community water supplies. If the model is valid, springs located within the 5 m drawdown contour are expected to dry out, which means that 16 springs and two village water supply springs will dry out by the end of mining; consequently, alternative water supply sources should be provided for these villages. In this regard, water extracted from the system as a result of dewatering activities can be used to replace the water demand arising from the drying of the springs/fountains. Hence, the impacts associated with dewatering activities can be minimized in terms of water supply.

Supplementary Information The online version contains supplementary material available at https://doi.org/10.1007/s10230-022-00877-4.

Acknowledgements This project was funded by IKA Mining Inc. through projects No. 11-03-09-02-00-36, No. 14-03-09-02-00-03, and No. 14-03-09-02-00-21 given to Middle East Technical University. The opinions, findings, conclusions, and recommendations expressed are those of the authors and do not necessarily reflect the views of IKA Mining Inc. The positive and constructive comments provided by the reviewers are greatly appreciated.

References

Adams R, Younger PL (2001) A strategy for modeling ground water rebound in abandoned deep mine systems. Groundwater 39(2):249–261

AMM (Asia Minor Mining) (2015) Geology of the Çeltikçi Project Area, corporate report

Anderson MP, Woessner WW, Hunt RJ (2015) Applied groundwater modelling, simulation of flow and advective transport. Elsevier, Amsterdam

Ardejani FD, Singh RN, Baafi E, Porter I (2003) A finite element model to: 1. Predict groundwater inflow to surface mining excavations. Mine Water Environ 22(1):31–38

Argunhan-Atalay C, Yazicigil H, Ekmekci M (2021) Assessment of performance of horizontal drains in an open pit mine in eastern Turkey. Environ Earth Sci 80:108

Aryafar A, Ardejani FD, Singh RN (2009) Numerical modeling of groundwater inflow from a confined aquifer into Sangan open pit mine, northeast Iran. Geomech Geoengin Int J 4(3):189–199

Bochenska T, Fiszer J, Kalisz M (2000) Prediction of groundwater inflow into copper mines of Lubin Glogow Copper District. Environ Geol 39(6):587–594

Booth CJ (2006) Groundwater as an environmental constraint of longwall coal mining. Environ Geol 49(6):796–803

Brouyere S, Orban PH, Wildemeersch S, Couturier J, Gardin N, Dassargues A (2009) The hybrid finite element mixing cell method: a new flexible method for modeling mine groundwater problems. Mine Water Environ 28(2):102–114

Brunetti E, Jones JP, Petitta M, Rudolph DL (2013) Assessing the impact of large-scale dewatering on fault-controlled aquifer systems: a case study in the Acque Albue basin (Tivoli, central Italy). Hydrogeol J 21(2):401–423

Castendyk DN, Eary T (eds) (2009) Mine pit lakes: characteristics, predictive modeling, and sustainability. Society for Mining, Metallurgy and Exploration (SME), Littleton

Connelly RJ, Gibson J (1985) Dewatering of the open pits at Letlhakane and Orapa diamond mines. Botswana Int J Mine Water 4(3):25–41

DHI-WASY (2015) FEFLOW (Finite Element subsurface FLOW simulation system) v. 7

Fernandez-Rubio R, Lorca DF (1993) Mine water drainage. Mine Water Environ 12(1):107–130

Fontaine RC, Davis A, Fennemore GG (2003) The comprehensive realistic yearly pi transient infilling code (CRYPTIC): a novel pit lake analytical solution. Mine Water Environ 22(4):187–193

Marinelli F, Niccoli WL (2000) Simple analytical equations for estimating ground water inflow to a mine. Groundwater 38(2):311–314

Morton KL, Mekerk FA (1993) A phased approach to mine dewatering. Mine Water Environ 12(1):27–34

Peksezer-Sayit A, Cankara-Kadioglu C, Yazicigil H (2015) Assessment of dewatering requirements and their anticipated effects on groundwater resources: a case study from the Caldag nickel mine, western Turkey. Mine Water Environ 34:122–135

Rapantova N, Grmela A, Vojtek D, Halir J, Michalek B (2007) Ground water flow modeling applications in mining hydrogeology. Mine Water Environ 26(4):264–270

SCS (Soil Conservation Services) (1964) SCS National Engineering Handbook. Section-4: Hydrology, updated. U.S. Dept of Agriculture, Washington, DC

Singh RN, Atkins AS (1985) Analytical techniques for the estimation of mine water inflow. Int J Min Eng 3:65–77

Thornthwaite CW (1968) An approach towards a rational classification of climate. Geogr Rev 38(1):55–94

Unsal B, Yazicigil H (2016) Assessment of open pit dewatering requirements and pit lake formation for the Kışladağ gold mine, Uşak, Turkey. Mine Water Environ 35:180–198

Williamson S, Vogwill RIJ (2001) Dewatering in the hot groundwater conditions at Lihir gold. Proc, IMWA Symp, Belo Horizonte, pp 1–15

Yazicigil H, Camur MZ, Yilmaz KK, Peksezer-Sayit A, Kahraman C (2015a) Development of groundwater flow model, design of dewatering system and assessment of ımpacts on groundwater resources for Çeltikçi Coal Basin. Middle East Technical University, Ankara, Turkey ((**unpublished) [in Turkish**])

Yazicigil H, Camur MZ, Yilmaz KK, Peksezer-Sayit A, Kahraman C (2015b) Water Supply Evaluation of Çeltikçi Coal Mine and Thermal Power Plant. Middle East Technical University, Ankara, Turkey ((**unpublished) [in Turkish**])

Yazicigil H, Camur MZ, Suzen ML, Yilmaz KK, Kahraman C, Peksezer-Sayit A (2014) Hydrogeological Characterization and Investigation of the Çeltikçi Coal Basin. Middle East Technical Univ, Ankara, (unpublished) [in Turkish]

Younger PL, Banwart SA, Hedin RS (2002) Mine water: hydrology, pollution. Springer, Berlin

Zaidel J, Markham B, Bleiker D (2010) Simulating seepage into mine shafts and tunnels with MODFLOW. Groundwater 48(3):390–400